TẠP CHÍ ISSN: 1859-316X, e-ISSN: 3093-3161
KHOA HỌC CÔNG NGHỆ HÀNG HẢI
JOURNAL OF MARINE SCIENCE AND TECHNOLOGY

DESIGN OF A NOVEL AUV HULL SHAPE FOR IMPROVING HYDRODYNAMIC PERFORMANCE USING CFD

PHAM THI THANH HUONG, LE MANH KIEN, NGO VAN HE*
School of Mechanical Engineering, Hanoi University of Science and Technology
**Corresponding email: he.ngovan@hust.edu.vn*
DOI: https://doi.org/10.65154/jmst.1155

Abstract
This topic presents the results of the design new hull form for an Autonomous Underwater Vehicle (AUV) to improve hydrodynamic performance, reduce resistance, and enhance operational energy efficiency. The proposed shape is designed based on biomimetic principles to optimize flow characteristics, improve flow attachment, and reduce wake intensity behind the AUV hull. A commercial Computational Fluid Dynamics (CFD) software is employed to evaluate the hydrodynamic performance of several proposed AUV hull configurations. The numerical analysis focuses on resistance components, pressure distributions, and flow-field structures under steady operating conditions. The results demonstrate that the newly developed hull form achieves a significant reduction in total resistance, together with a more uniform pressure distribution and reduced flow separation in the stern region. These improvements contribute to improved hydrodynamic performance, reduced resistance characteristics, and enhanced operational efficiency of the AUV. The study also demonstrates the applicability of CFD as an effective numerical approach for analyzing and optimizing AUV hull configurations, thereby providing useful insights for the design and development of high-performance underwater vehicles operating under complex marine conditions.

Keywords: *Hull form, AUV, CFD, resistance, hydrodynamic performance.*

1. Introduction

Autonomous Underwater Vehicles (*AUVs*) have emerged as essential instruments for a wide range of military and civilian tasks, such as seabed mapping, marine archaeology, environmental monitoring, and offshore oil and gas exploitation. These vehicles are designed to perform complex underwater missions autonomously, thereby improving operational efficiency and reducing risks associated with human intervention in hazardous environments [1, 2, 3]. Although AUVs typically operate at considerable depths to avoid environmental disturbances, operating at the free surface is mandatory for critical mission phases, including data transfer, Global Positioning System (*GPS*) localization corrections, and vehicle retrieval [4, 5, 6]. In particular, free-surface effects induce added wave resistance and pressure distributions around the hull, leading to increased resistance and unsteady hydrodynamic forces [7-9]. These phenomena can significantly affect the hydrodynamic performance of the vehicle, including its stability, maneuverability, and resistance. Therefore, free surface effects should be considered in the analysis and design of AUVs.

The demand for improved energy efficiency has prompted significant study into hull shape optimization, predominantly employing CFD tools as a cost-effective substitute for experimental testing. Divsalar (2019) investigated the influence of nose and tail geometries as well as length-to-diameter ratios using the SUBOFF bare hull model, while Sener and Aksu (2022) examined the effects of head-form variations on resistance and flow characteristics, both using ANSYS Fluent [3, 9]. Their findings confirmed that hull geometry significantly affects both pressure and friction resistance components. Additionally, Gao, Wang et al. (2016) and Hou, Liang, and Mu (2018) presented an optimization platform for AUV hull shapes, successfully implemented multi-island genetic algorithms (MIGA) to refine Myring-type geometries for improved reliability and endurance [4, 6, 9-11]. More recently, Roham Lavimi, Alla Eddine Benchikh Le Hocine et al. (2024) developed a CFD-driven optimization framework focusing on nose and tail geometries, showing that systematic shape modifications can improve hydrodynamic performance [13]. However, the majority of these studies assume fully submerged operation in an infinite fluid domain.

Several numerical studies have investigated the

TẠP CHÍ ISSN: 1859-316X, e-ISSN: 3093-3161
KHOA HỌC CÔNG NGHỆ HÀNG HẢI
JOURNAL OF MARINE SCIENCE AND TECHNOLOGY

hydrodynamic performance of AUVs moving near the free surface, with primary emphasis on the variation of resistance, lift force, and flow around hull in the different depths and operating conditions. Mansoorzadeh and Javanmard (2014) presented results on research of the free surface effect on the AUV's hydrodynamic performance utilizing ANSYS CFX [10]. This investigation demonstrated that the AUV's resistance became greater near the free surface due to enhanced wave-making resistance. Mitra et al. (2019) examined the influence of free-stream turbulence on the flow dynamics over an AUV at different depths and attack angles [11]. Several studies reported that, when the AUV moves in the flow separation condition, the pressure and hydrodynamic forces acting on the AUV hull are reduced. Tian et al. (2019) analyzed the effect of the free surface on the AUV's resistance in the wave condition. [13-17]. The research was done on different Reynolds numbers, the height of the wave, and the drafts of the AUV. The lift exhibited significant fluctuations in the presence of waves, while the AUV's resistance increased with the wave height. Jin Guo et al. (2023) used CFD computations to investigate the hydrodynamic performances of a disk-shaped AUV moving near the free surface. The results demonstrated that wave parameters, cruising depth, and velocity distribution around the AUV had an effect on the AUV's resistance[7]. Ahmad, Hasnan et al. (2025) investigated the hydrodynamic performance acting on the DARPA SUBOFF AUV model in both independent hull and the hull with fully appended hull configurations, concentrating on hydrodynamic forces near the free surface [1]. Most studies focus on existing benchmark geometries and do not systematically investigate hull shape modifications to reduce free-surface-induced resistance.

In this study, several AUV hull configurations are investigated to evaluate their hydrodynamic performance. Based on the original hull, modified hull designs are developed and analyzed to examine the effects on the AUV's hydrodynamic performance, as well as the resistance, pressure distribution, and flow around the AUV.

2. AUV model used for CFD simulation

In this section, an AUV model with an integrated fin–hull configuration has been developed by using CFD. The overall geometry of the proposed AUV is illustrated in Figure 1. The principal dimensions of the AUV are listed in Table 1.

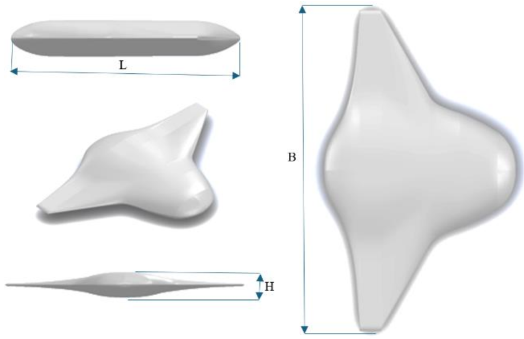

Figure 1. Hull shape of the model AUV-1

Table 1. Principal dimensions of the AUV-1

Parameter	Value	Unit
Length, L	1.40	m
Beam, B	2.12	m
Height, H	0.22	m
Displacement Volume, V	0.17	m^3
Block coefficient, C_b	0.289	-

The two different hull forms are developed for the AUV. The geometrical features of the proposed AUV's hull are shown in Figures 2 and 3, and their principal dimensions are provided in Tables 2, 3.

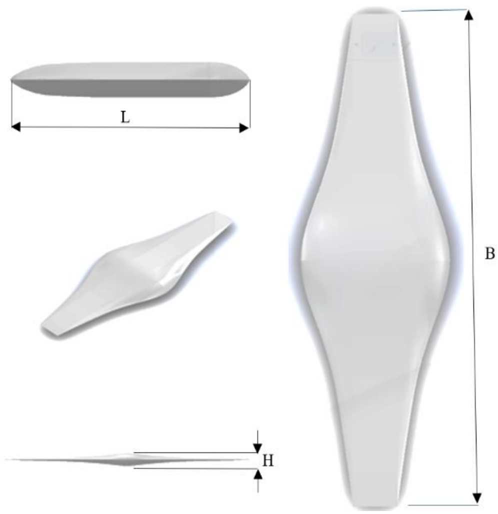

Figure 2. Hull shape of the AUV-2

Table 2. Principal Dimensions of the AUV-2

Parameter	Value	Unit
Length, L	1.20	m
Beam, B	3.52	m
Height, H	0.16	m
Displacement Volume, V	0.18	m^3
Block coefficient, C_b	0.432	-

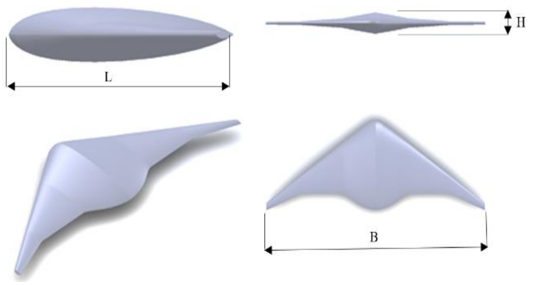

Figure 3. Hull shape of the AUV-3

Table 3. Principal Dimensions of the AUV-3

Parameter	Value	Unit
Length, L	1.40	m
Beam, B	4.02	m
Height, H	0.31	m
Volume of displacement, V	0.22	m^3
Block coefficient, C_b	0.173	-

3. CFD simulation of the hydrodynamic performance of the AUV

In this study, the proposed AUVs are simulated by using the CFD software STAR-CCM+. The computational domain, mesh, and setup boundary condition in the simulations are illustrated in Figure 4.

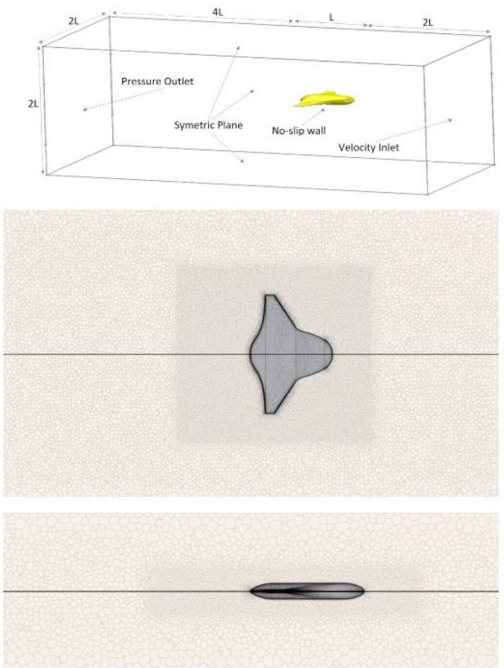

Figure 4. Computed domain, mesh, and setup conditions

In CFD analysis, the accuracy and stability of the numerical results are strongly dependent on the computational setup, including the computational domain size, mesh quality, near-wall treatment, and applied boundary conditions. Therefore, the numerical model used in this study was established based on recommended CFD practices, published literature, and previous experience in hydrodynamic simulations of AUVs. The mesh convergence behavior and grid independence assessment are presented in Figure 5 to demonstrate the reliability of the computational mesh adopted in this work.

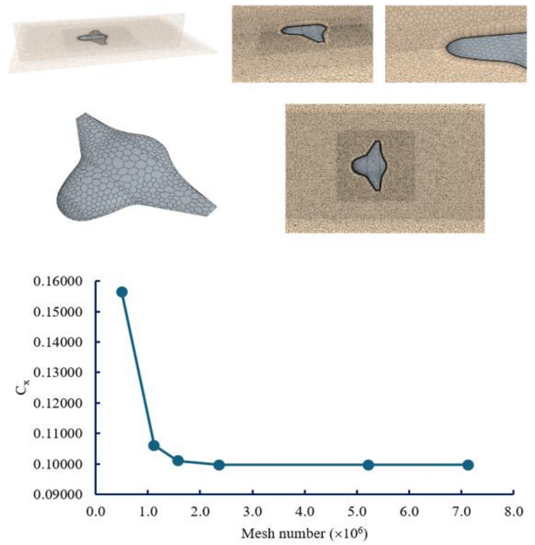

Figure 5. Resistance coefficient acting on the AUV-1 for different mesh numbers

The results, as shown in Figure 5, show the resistance acting on the model AUV-1 in the different mesh numbers. The results show that the resistance coefficient converges as the mesh number increases. From the mesh number higher than 2 million grids, the resistance coefficient acting on the AUV-1 is constant. The results indicate that mesh independence has been achieved. In the research, all computed cases are done with the mesh number up to 2.56 million.

In this research, all models are computed by the CFD in the same conditions and compered at other to clearly the effect of hull shape on the hydrodynamic performance of the AUV. The solution has used the Reynolds-Averaged Navier–Stokes (*RANS*) approach. The turbulent viscous model k–ε standard model was used in the computation [3, 5, 12]. A velocity inlet is set up at the inlet, and a pressure outlet is set up at the outlet of the computed domain. The condition of a no-slip wall is set up for the wall and the AUV's surface. The simulations are conducted for inlet velocity in the range of 1.0 to 3.0m/s, corresponding to Reynolds numbers of 1.57×10^6 to 4.71×10^6.

TẠP CHÍ ISSN: 1859-316X, e-ISSN: 3093-3161
KHOA HỌC CÔNG NGHỆ HÀNG HẢI
JOURNAL OF MARINE SCIENCE AND TECHNOLOGY

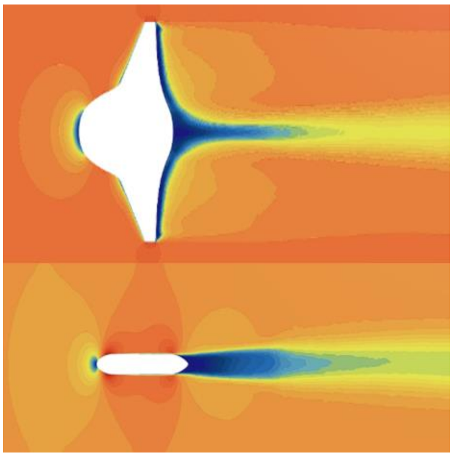

a) AUV-1

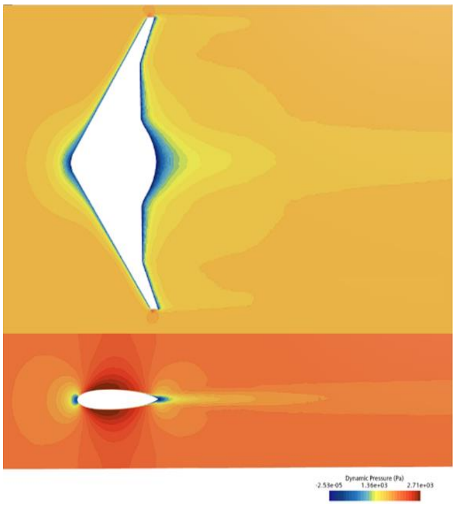

b) AUV-2

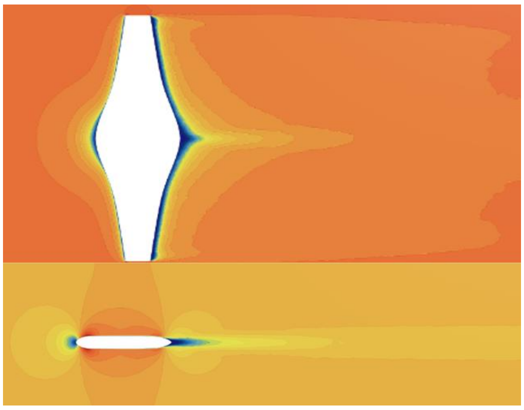

c) AUV-3

Figure 6. Distribution of the dynamic pressure around the AUV, at R_e=3.14×10^6

The results, as shown in Figures 6 and 7, show the dynamic pressure distribution around the AUVs in the different hull shapes. The results show clearly effect of hull shapes on pressure distribution around the AUVs.

The results in Figure 6 clearly illustrate the effect of hull shape variation on the dynamic pressure distribution around the AUV. High-pressure regions are represented by red and yellow contours, whereas blue regions indicate zones of low dynamic pressure in the surrounding flow field.

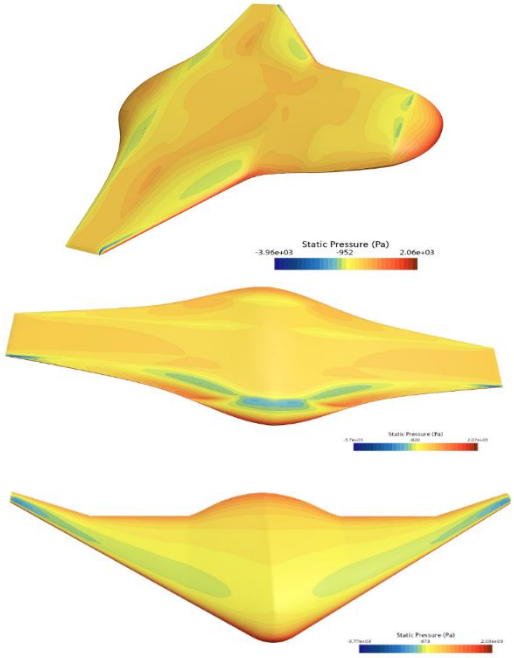

Figure 7. Pressure distribution over the hull surface of the AUV, at R_e=3.14×10^6

Figure 7 shows the distribution of the pressure over the hull surface of the AUVs. The figure clearly shows the differences in pressure concentration regions associated with the various hull shapes. In the results, red and yellow regions represent zones of relatively high static pressure acting on the vehicle surfaces, particularly near the frontal and curved sections of the hulls.

4. CFD results of AUV's hydrodynamic force

In this section, the hydrodynamic forces acting on the AUVs are analyzed based on the CFD. A comparative assessment of the force components is conducted to clearly understand the effect of hull shape on the hydrodynamic performance of the AUVs. Figure 8 shows the AUV's hydrodynamic force coefficients, C_x, C_y, and C_z.

In this research, the AUV's hydrodynamic force coefficients are defined as follows:

$$C_x = \frac{F_x}{\frac{1}{2}\rho S_x V^2};\ C_y = \frac{F_y}{\frac{1}{2}\rho S_y V^2};\ C_z = \frac{F_z}{\frac{1}{2}\rho S_z U V^2} \quad (1)$$

Where F_x, F_y, and F_z denote the hydrodynamic force in their respective directions acting on the AUVs, and S_x, S_y, and S_z are the reference frontal projected area of the AUVs.

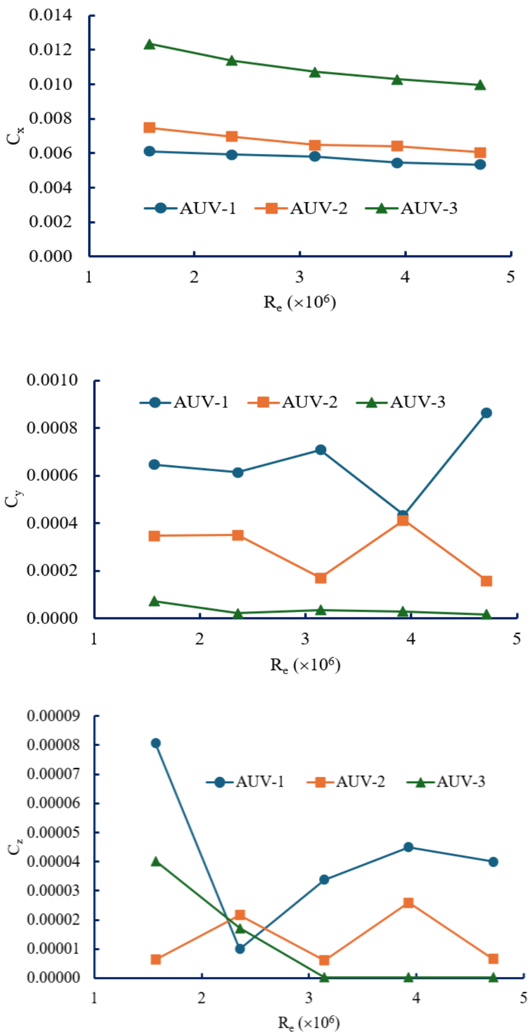

Figure 8. Dynamic force coefficient acting on the AUVs

The results, as shown in Figure 8, show clearly the effect of the AUV's shapes on the hydrodynamic forces. In the results, resistance acting on the model AUV-1 is the lowest resistance coefficient C_x in compared with those of the models AUV-2 and AUV-3. The difference of the resistance coefficient among the models is up to 50,49% at R_e=1.57×10^6. The results show that the effect of the AUV shapes on the resistance coefficient is clear.

These results show that effective hull design optimization can lead to substantial resistance reduction and improved overall efficiency of AUV operation. The corresponding quantitative values of the hydrodynamic force components for the investigated configurations are summarized in Tables 4–6.

Table 4. The AUV-1's hydrodynamic force

R_e×10^6	C_x	C_y	C_z
1.570	0.006118	0.000646	0.000081
2.356	0.005922	0.000614	0.000010
3.142	0.005792	0.000707	0.000034
3.928	0.005451	0.000434	0.000045
4.713	0.005351	0.000865	0.000040

Table 5. Hydrodynamic force acting on the AUV-2

R_e×10^6	C_x	C_y	C_z
1.570	0.00747	0.00035	0.000006
2.356	0.00697	0.00035	0.000022
3.142	0.00648	0.00017	0.000006
3.928	0.00640	0.00041	0.000026
4.713	0.00605	0.00016	0.000006

Table 6. Hydrodynamic force acting on the AUV-3

R_e×10^6	C_x	C_y	C_z
1.570	0.012357	0.000071	0.000040
2.356	0.011392	0.000023	0.000017
3.142	0.010736	0.000034	0.000000
3.928	0.010288	0.000028	0.000000
4.713	0.009961	0.000016	0.000000

Tables 4-6 show the AUV's hydrodynamic force coefficients in the same computed conditions. The results show that the AUV's resistance coefficient C_x clearly changes following the different shapes.

Table 7. Comparison of the AUV's hydrodynamic force

R_e×10^6	F_x, %	F_y, %	F_z, %
AUV-2			
1.570	18.10	46.22	92.30
2.356	15.01	43.02	53.99
3.142	10.63	76.09	82.18
3.928	14.86	5.13	42.29
4.713	11.61	81.77	83.81
AUV-3			
1.570	50.49	89.01	50.17
2.356	48.01	96.33	73.58
3.142	46.06	95.19	99.43
3.928	47.02	93.50	99.62
4.713	46.28	98.13	99.48

Table 7 presents the comparative variations in hydrodynamic force components of the AUV-2 and AUV-3 with those of the AUV1, configurations relative to the different Reynolds numbers. The results

TẠP CHÍ ISSN: 1859-316X, e-ISSN: 3093-3161
KHOA HỌC CÔNG NGHỆ HÀNG HẢI
JOURNAL OF MARINE SCIENCE AND TECHNOLOGY

indicate that the modified hull influences the hydrodynamic characteristics of the AUVs, particularly for the AUV-3 configuration.

For AUV-2, the variation in the longitudinal force coefficient component C_x remains relatively moderate, ranging from approximately 10.63% to 18.10% across the investigated Reynolds number range. The results of the hydrodynamic forces of the transverse and vertical force components (C_y and C_z) show larger fluctuations, especially at higher Reynolds numbers. The results indicate that the developed AUV's shape affects the flow and pressure distribution around the AUVs.

The results of the hydrodynamic force acting on the AUV-3 configuration shows substantially larger variations in all direction axis hydrodynamic force components compared with the original hull. The resistance acting on the AUV-3, C_x increases up to (46.06–50.49)%, while the C_y and C_z components show variations exceeding up to 90% as shown in Table 7. These results suggest that the hull shape of the AUV-3 has stronger alterations in the surrounding flow field around the AUV. The results demonstrate that the hull shape of the AUV-3 is more significant pressure distribution and wake effects. The results confirm that the developed AUV's hull shape has a pronounced influence on the hydrodynamic performances. In the results as shown, AUV-2 shows comparatively more stable hydrodynamic performances, whereas AUV-3 produces the largest deviations in force components due to its more substantial hull shape modification.

5. Conclusions

By using the CFD, the hydrodynamic performance of the AUV with the different hull shapes is investigated. Based on the CFD results of the comparison among the AUV models, the effects of hull shape on hydrodynamic performance are found.

The results of the hydrodynamic performance acting on the proposed AUVs show that hull shape has a significant effect on the AUV's hydrodynamic performance. The resistance acting on the AUV is reduced by up to 50.49% compared to other proposed models, as shown.

The results of the hydrodynamic performance, such as the flow and pressure distribution around the AUV, show that hull shape drastically effect on flow and pressure around the AUVs. The reason for increasing resistance can be the changing pressure and flow distribution around the AUVs.

Acknowledgments

This research is funded by Hanoi University of Science and Technology (HUST) under project number T2025-PC-038. The authors would like to warmly thank you for your support.

REFERENCES

[1] Ahmad, M. S., et al. (2025), *Numerical simulation of hydrodynamic forces on an underwater vehicle near the free surface,* Journal of Applied Fluid Mechanics, Vol.18(9).

[2] Chen, X., et al. (2023), *Multi-objective shape optimization of autonomous underwater vehicle by coupling CFD simulation with genetic algorithm*, Ocean Engineering, Vol.286.

[3] Divsalar, K. (2019), *Improving the hydrodynamic performance of the SUBOFF bare hull model: A CFD approach,* Acta Mechanica Sinica, Vol.36(1), pp.44-56.

[4] Gao, T., et al. (2016), *Hull shape optimization for autonomous underwater vehicles using CFD*, Engineering Applications of Computational Fluid Mechanics, Vol.10(1), pp.599-607.

[5] Hong, L., et al. (2021), *Numerical investigation on hydrodynamic performance of a portable AUV*, Journal of Marine Science and Engineering, Vol.9(8).

[6] Hou, Y. H., Liang, X., & Mu, X. Y. (2018), *AUV hull lines optimization with uncertainty parameters based on six sigma reliability design*, International Journal of Naval Architecture and Ocean Engineering, Vol.10(4), pp.499-507.

[7] Guo, J., et al. (2023), *Numerical research on hydrodynamic characteristics of the disk-shaped autonomous underwater vehicle near free surface*, Ocean Engineering, Vol.288.

[8] Kaya, K. D., et al. (2020), *Determination of operating parameters of an AUV following a preplanned trajectory using hydrodynamic analysis data*, Ocean Engineering, Vol.217.

[9] Liu, H.-L., & Huang, T. T. (1998), *Summary of DARPA SUBOFF experimental program data*, Technical Report.

[10] Mansoorzadeh, S., & Javanmard, E. (2014), *An investigation of free surface effects on resistance and lift coefficients of an autonomous underwater vehicle (AUV) using computational and experimental fluid dynamics methods*, Journal of

Fluids and Structures, Vol.51, pp.161-171.

[11] Mitra, A., Panda, J. P., & Warrior, H. V. (2019), *The effects of free stream turbulence on the hydrodynamic characteristics of an AUV hull form*, Ocean Engineering, Vol.174, pp.148-158.

[12] Panda, J. P., Mitra, A., & Warrior, H. V. (2020), *A review on the hydrodynamic characteristics of autonomous underwater vehicles,* Proceedings of the Institution of Mechanical Engineers, Part M: Journal of Engineering for the Maritime Environment, Vol.235(1), pp.15-29.

[13] Lavimi, R., et al. (2024), *Hull shape optimization of autonomous underwater vehicles using a full turbulent continuous adjoint solver*, Ocean Engineering, Vol.312.

[14] Randeni, P. S. A. T., et al. (2015), *Numerical investigation of the hydrodynamic interaction between two underwater bodies in relative motion*, Applied Ocean Research, Vol.51, pp.14-24.

[15] Sener, M. Z., & Aksu, E. (2022), *The effects of head form on resistance performance and flow characteristics for a streamlined AUV hull design*, Ocean Engineering, Vol.257.

[16] Tian, W., et al. (2017), *Layout optimization of two autonomous underwater vehicles for resistance reduction with a combined CFD and neural network method*, Complexity, Vol.2017, pp.1-15.

[17] Tian, W., Song, B., & Ding, H. (2019), *Numerical research on the influence of surface waves on the hydrodynamic performance of an AUV*, Ocean Engineering, Vol.183, pp.40-56.

Received:	13/05/2026
Revised :	25/05/2026
Accepted:	28/05/2026